Journal of Hazardous Materials 178 (2010) 341–348

Contents lists available at ScienceDirect

Journal of Hazardous Materials

journal homepage: www.elsevier.com/locate/jhazmat

Study of the behaviour of different NF membranes for the reclamation of a secondary textile effluent in rinsing processes

Amparo Bes-Piá*, Beatriz Cuartas-Uribe, Jose-Antonio Mendoza-Roca, M.I. Alcaina-Miranda

Department of Chemical and Nuclear Engineering, Universidad Politécnica de Valencia, Camino de Vera s/n, Valencia 46022, Spain

ARTICLE INFO

Article history:
Received 25 June 2009
Received in revised form 18 January 2010
Accepted 19 January 2010
Available online 25 January 2010

Keywords:
Volume concentration factor (VCF)
Fouling
Textile industry
Nanofiltration
Reuse

ABSTRACT

More demanding legal regulations for the wastewater disposal and water scarcity make necessary wastewater reuse in the industry. In particular, textile industry generates large amounts of wastewater with a high concentration of pollutants. Even though present biological or physical–chemical treatments are broadly in place, the quality of the final effluent is not good enough to allow its direct reuse. Consequently, a complementary membrane process is required in order to improve wastewater characteristics. In this work, six NF membranes were tested at different volume concentration factors in order to select the most appropriate one. The main studied criteria were the permeate quality for its reuse in the textile processes and the minimum membrane fouling effect. The different results obtained for the tested membranes were explained by membrane characterization parameters as contact angle, roughness and size exclusion. Taking these factors into consideration, TFC-SR2 has shown the overall best results because of the high permeate flux and the minimum fouling (in terms of the normalised flux reduction).

1. Introduction

In the Mediterranean areas, wastewater treatment plants in the industry are currently being upgraded due to severe legal regulations and the necessity of water reuse. Specifically, textile industry processes require high water usage; thereby a large amount of wastewater is generated.

Effluents from textile mills show different characteristics depending on the production processes. For a typical printing, dyeing and finishing textile factory, the wastewater is characterized by alkaline pH values (11.0–12.5), suspended solids (SS) between 200 and 400 mg L^{-1}, chemical oxygen demand (COD) values from 1500 to 2500 mg L^{-1}, presence of colour and conductivity values varying between 2 and 5 mS cm^{-1} [1].

Currently, the most common raw textile wastewater treatments are based on biological or physical–chemical processes with previous screening and pH adjusting steps. Biological treatment by activated sludge offers high efficiencies in COD removal, but does not completely eliminate the colour of the wastewater due to the azo dyes nature [2]. Physical–chemical treatment allows reducing dissolved, suspended, colloidal, nonsettleable matter and colour from the wastewater by chemical coagulation–flocculation followed by gravity settling. However, the main drawback is the sludge management due to the high amount produced and the metals content, mainly Fe^{+3} and Al^{+3}.

In previous studies, effluents coming from textile wastewaters were treated with physical–chemical and biological treatments. The best results obtained for COD in the final effluent varied between 448 and 65 mg L^{-1}, respectively, whereas SS values were 205 and 40 mg L^{-1} for the same treatments [1,3].

If advanced technologies like membrane processes are combined with conventional treatments, the characteristics of the treated wastewater can be appropriate for its reuse [4]. Specifically, nanofiltration (NF) is able to separate organic compounds and bivalent ions which are still present in the treated water. Nevertheless, its reuse depends on the final quality or purity of the water, which will be function of the textile process.

NF is a membrane process that has been applied to different industrial effluents. In this way, Boussu et al. [5] applied NF to recycle water from the carwash industry. Mänttäri et al. [6] carried out the study of the treatment by NF of the biologically treated pulp and paper mill wastewaters. In tanneries, some authors have studied the NF application for chromium (III) and sulphate removal for water reuse in the pickling and tanning processes [7–9].

In the particular case of the textile industry, NF has been studied as treatment for partial streams as well as for the global wastewater. For the first case, Qin et al. [10] studied the feasibility of reuse water from a specific dying process by NF. Authors tested three different membranes (Desal-5 from Osmonics, NE-70 from Saehan y TS-40NF from Trisep). For the best tests, colour removal was 99% and the water recovery was around 70%. Akbari et al. [11] tested a new

* Corresponding author. Tel.: +34 96 387 70 07; fax: +34 96 387 76 39.
E-mail address: mbespia@iqn.upv.es (A. Bes-Piá).

0304-3894/$ – see front matter © 2010 Elsevier B.V. All rights reserved.
doi:10.1016/j.jhazmat.2010.01.085

NF membrane for the treatment of coloured textile dye effluents. It was found an acceptable performance in terms of flux and rejection that was higher than 96% for dyes. Koyuncu et al. [12] reported their results after applying NF to a synthetic wastewater simulating the dyeing wastewater (dye and sodium chloride) and studied the membrane fouling. They concluded that the principal cause of flux decline at low salts concentration was the cake layer formation of dye molecules on membrane surface. Similar studies have been reported in this way [13–17].

On the other hand, other research works are also focused on water reuse but considering the total effluents generated in the textile industry. Sahinkaya et al. [18] reported results of NF experiments with biologically treated textile wastewaters. The membrane used was NF 270 and the main outcomes were a flux between 31 and 37 $L\,m^{-2}\,h^{-1}$ at 5 bar and a 65% of conductivity removal. The results also showed high rejection values in terms of COD (80–100%) and colour (almost 100%). In the same direction, studies with a combination between biological treatment and membranes have been carried out [3,19]. Other authors treated directly the textile effluents using membranes. Thus, Barredo-Damas et al. [20] and Fersi and Dhahbi [21] applied UF process as pre-treatment of NF membranes in order to reduce fouling problems.

The main objective of this study was to select the most appropriate NF membrane to reuse the secondary effluent from a textile mill wastewater treatment plant in the rinsing process. For that, it was studied the influence of a high range of volume concentration factors on the membrane fouling and the final permeates quality: colour, conductivity, COD and hardness (in terms of calcium and magnesium).

2. Materials and methods

2.1. Textile industry

The textile industry plant of the study mainly consists of printing and dying processes. In these processes, the use of substances such as NaCl and Na_2CO_3 is required to favour the aggregation of dye ions on the fibre to fix the dyestuffs. Currently, the process water is supplied from a well. However, in order to reduce the hardness of this water a softening step (ion exchange beds) is applied.

These processes require high amount of water. Thus, the textile mill studied generates daily 2500 m^3 of wastewater with a mean organic concentration of 3000 mgCOD L^{-1}. About 10% of the total wastewater comes from the dying and printing residual baths whereas 85% comes from rinsing. Hence, water recycling in rinse process is the key point for saving fresh water in this industry.

The wastewater treatment plant located in the textile industry is divided into three steps: pre-treatment, biological and sludge treatments. The first one includes an equalization tank and two screenings for different particle sizes. The secondary treatment consists in a conventional activated sludge treatment with a total hydraulic retention time of 2 days. The overall efficiency of this process is higher than 90% in terms of total organic matter reduction. This step includes a flotation stage to separate the sludge from the clarified water. The sludge generated is dehydrated by a band filter and finally the sludge volume is minimized by a thermal drying system.

2.2. Feed water characterization

The feed of the NF membranes corresponded with the biological treated wastewater from the textile wastewater treatment plant (TWWTP). For the experiments, different samples of this effluent were taken and characterized during six months. The analysed parameters were conductivity, pH, colour, chemical oxygen demand (COD), suspended solids (SS), turbidity and main ions concentrations. Besides, the particle size distribution (PSD) of the feed samples was measured.

2.3. Membrane pilot plant description

Membrane experiments were performed in a pilot plant designed in the Universidad Politécnica de Valencia (Fig. 1). It is equipped with a pressure vessel for one spiral wound membrane module of 2.5″ diameter. The feed tank included a stirrer to homogenize the feed and a level switch that enabled continuous operation. The temperature was kept constant by a cooling system. An 8 μm pre-filter was placed upstream in order to reduce the pass of particles into the system and to minimize the membrane fouling. Two manometers at each side of the membrane module were used to measure the transmembrane pressure (TMP). A flow meter was located in the concentrate stream to measure its volumetric flow rate. Moreover a valve placed next to the flow meter was used to regulate the TMP.

The NF membranes tested were TFC-SR2 from KOCH, ESNA from Hydranautics, NF270 from DOW CHEMICAL and DS-5 DK, DS-5 DL and Duraslick from General Electric. The main specifications of these spiral wounded membrane elements provided by the manufacturers, literature and authors are shown in Table 1.

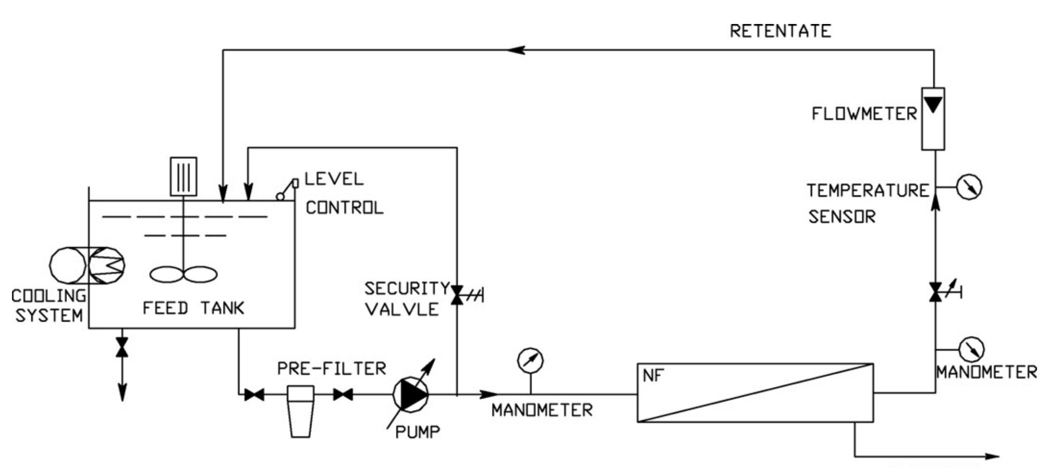

Fig. 1. Experimental set-up for NF experiments.

Table 1
Main membranes characteristics according to manufacturers, literature data and authors.

Characteristic	DS-5 DK	DS-5 DL	NF270	TFC-SR2	ESNA 1 LF	Duraslick
Manufacturer	GE	GE	Dow Chemical	Koch–Fluid System	Hydranautics	GE
Type	TFC	TFC	TFC	TFC	CP	TFM
Support material	PS	PS	PS	PS	PS	PS
Surface material	PA	PA	PPZ	PA	PPZ	PA
Membrane area (m^2)	2.51	2.60	2.60	2.50	2.60	2.20
pH operating range	2–11	2–12	2–11	4–9	3–10	2–11
Maximum pressure (MPa)	3.45	4.10	4.10	2.41	2.10	4.13
Maximum temperature (°C)	50	50	45	45	45	50
% R $MgSO_4$	98.5	96.0	>97.0	97.0	N.A.	96.0
Cut-off (Da)	150–300	150–300	200–300	200–300	N.A.	N.A
Contact angle (°)	17.0 [22]	49.4 [23]	51.4 [24]	13.1 ± 6.4 [25]	60.0 [26]	30.0
Zeta potential (mV)	−5.0 (pH 7) [27]	−17.0 (pH 6) [28]	−24.7 (pH 8) [29]	−21.8 (pH 8–10) [25]	−10.0 (pH 9) [26]	N.A
Isoelectric point	4.1 [30]	3.0 [31]	3.3 [30]	4.7 [32]	4.9 [26]	N.A.
Roughness (nm)	9.50 [33]	9.50–13.30 (pH 3–10) [28]	19.80 [34]	0.45[a]	55.00 [34]	N.A.
Pore diameter size (nm)	0.92[a]	0.94[a]	0.84 [29] 0.82[a]	1.28 [35]	0.60 [36]	0.80–1.20
Thickness (μm)	2.95[a] 2.59 [37]	2.84[a] 2.54 [37]	1.87[a]	0.15–0.20	N.A.	0.20

TFC: thin film composite; CP: composite polyamide; TFM: thin film membrane; PPZ: polypiperazine amide; PA: polyamide. N.A.: not available.
[a] Determined by authors.

2.4. Permeability coefficients

At the beginning, permeability coefficients were determined with distilled water for all membranes. The operating conditions for these tests were a feed flow rate of 400 L h^{-1}, a temperature of 23 °C and TMP between 0.5 and 1.5 MPa. The flux measured with distilled water was labelled as J_{CW}.

The permeability coefficient was also determined in order to study the membrane fouling. Thus, at the end of each experiment, the membranes were rinsed with distilled water (at TMP = 0 and high feed flow rate) and the membrane permeability test was checked again.

2.5. NF experiments for the secondary textile effluent

It was studied the influence of different VCF (1.0, 1.2, 1.5, 2.0, 3.0 and 6.0) on the wastewater permeate flux, J_{WW} (L m^{-2} h^{-1}), R_{COD} (%), hardness rejection in terms of calcium and magnesium ($R_{hardness}$, %), R_{salts} (%) and R_{colour} (%). Permeate fluxes, $J_{WW,}$ and ions were measured with accuracies of ±0.2% and ±1.0%, respectively. For the COD measurements, accuracies were ±6 or ±11 mg L^{-1} depending on the measured COD range (10–150 or 50–500 mg L^{-1}).

The VCF was calculated by the Eq. (1)

$$VCF = \frac{V_F}{V_F - V_P} \quad (1)$$

where V_F and V_P were the initial feed volume and the total withdrawn permeate volume, respectively.

For the last test (VCF = 6), the feed volume was 10 L. It has to be highlighted that a VCF = 6 implies a total feed volume reduction of 83% and then a little rejected volume (V_R) to be managed.

The operating conditions were 400 L h^{-1} of feed flow rate and a temperature of 23 °C. For the membranes TFC-SR2, ESNA, Duraslick, DS-5 DK, NF270 and DL-5 DL, the applied TMP at VCF = 1 were 0.16, 0.55, 0.53, 0.91, 0.45 and 0.56 MPa, respectively. These TMP values were established to get an initial recovery of 15% for each membrane element and these TMP were kept constant for all tested VCF. The term recovery is defined as the fraction of the feed flow which passes through the membrane. Membranes suppliers do not recommend working at values higher than 15% of recovery for each membrane element. The feed and permeate streams were analysed when the steady state was achieved for each VCF in order to calculate the permeate fluxes and rejections.

The initial feed volume was 60 L. At each VCF both permeate and retentate streams were recycled to the feed tank. Once the NF process had reached the steady state and samples from permeate and retentate streams were taken, the VCF was changed by withdrawing 10 L of permeate, which were stored in a separated tank.

The rejection percentage for a specific solute was calculated by the Eq. (2)

$$R(\%) = \frac{C_F - C_P}{C_F} \cdot 100 \quad (2)$$

where C_P and C_F were the component concentration in the permeate and feed stream, respectively.

The membrane flux was calculated using the Eq. (3)

$$J = \frac{Q_P}{A_m} \quad (3)$$

where Q_P was the feed flow rate of the permeate stream and A_m the membrane surface.

2.6. Analytical methods

COD analyses were carried out in test tubes from MERCK (reference 1.14540.0001 for the COD range from 10 to 150 mg L^{-1} and reference 1.14690.0001 for the COD range from 50 to 500 mg L^{-1}). These tubes contain the required reagents for the oxidation (potassium dichromate, sulphuric acid and silver sulphate). The COD concentrations were measured by spectrophotometry using the Spectroquant Nova 60 from MERCK. The main ions and the suspended solids were determined according to the Standard Methods [38]. These analyses were replicated. Conductivity and pH were measured with CRISON instruments and turbidity with D-112 apparatus from DINKO. The colour was calculated using the Eq. (4)

$$Colour = \frac{\lambda_{436}^2 + \lambda_{525}^2 + \lambda_{620}^2}{\lambda_{436} + \lambda_{525} + \lambda_{620}} \quad (4)$$

where λ represents the absorbance values measured at three different wave lengths in the visible range (436 nm, 525 nm and 620 nm) [39].

Table 2
Feed water characterization and water reuse criteria.

Parameter	Feed	Reuse criteria[a]
Conductivity (mS cm^{-1})	2.6–2.8	<2.5
pH	7.6–7.8	6.0–8.0
Colour	0.39–0.54	0
Turbidity (NTU)	8.2–12.6	1.0
COD (mg L^{-1})	200–315	25
TSS (mg L^{-1})	15–46	0
TDS (mg L^{-1})	1456–1568	<1250
Hardness (mg L^{-1} as $CaCO_3$)	133–171	10
Ca^{+2} (mg L^{-1})	40–47	–
Mg^{+2} (mg L^{-1})	8–13	–
CO_3^{-2} (mg L^{-1})	96–96	–
HCO_3^{-2} (mg L^{-1})	800–1000	–
SO_4^{-2} (mg L^{-1})	124–176	–
Cl^- (mg L^{-1})	200–365	–
Na^{+1} (mg L^{-1})	179–190	–
K^{+1} (mg L^{-1})	54–67	–

TSS total suspended solids; TDS total dissolved solids; NTU nephelometric turbidity unit.
[a] According to the textile industry of this study.

The particle size distribution (PSD) was measured using Mastersizer 2000 from Malvern Instruments. The roughness and the pore size of the TFC-SR2 membrane surface were determined by atomic force microscope (AFM) by Digital Instruments Nanoscope IIIA from USA. The surface area of the membrane for the analysis was 2 μm × 2 μm.

3. Results and discussion

3.1. Secondary textile effluent characterization

According to the information supplied by the textile industry management team, the problems for the direct reuse of the effluent from the TWWTP in the rinsing process are mainly its high organic load and its colour. Besides, divalent ions that cause water hardness also avoid a direct effluent reuse, since they reduce the rinse process efficiency.

As shown in Table 2, the wastewater conductivity is high (near 3 mS cm^{-1}) mainly due to the chlorides which are added as salts to fix the dyestuffs during the printing and dying process. Regarding pH, wastewater is practically neutral due to a pH adjusting step previous to the conventional activated sludge treatment. The colour measurement has been also included. As it can be seen, the colour value is low as a consequence of the dilution with all the streams rather than due to the biological treatment itself. As mentioned before, the type of dye use is not totally biodegradable (azo type) [40]. The COD values are around 260 mg L^{-1} and the variation of turbidity (8–13 NTU) is not significant.

Table 3
Permeability membrane values before tests.

Membrane	Regression line	R^2	TMP (MPa)	J_{cw} (L m^{-2} h^{-1})[a]
TFC-SR2	J_{cw} = 179.70·TMP	0.99	0.16	28.75
NF270	J_{cw} = 88.15·TMP	1.00	0.45	39.67
Duraslick	J_{cw} = 69.87·TMP	0.98	0.53	36.68
DS-5 DL	J_{cw} = 65.86·TMP	1.00	0.56	36.88
ESNA	J_{cw} = 59.87·TMP	0.99	0.55	32.93
DS-5 DK	J_{cw} = 31.11·TMP	0.98	0.91	28.31

[a] J_{cw} calculated at TMP showed.

In Fig. 2 it can be observed the PSD analysis. Before the micro-filtration, *d* (90) (90% percentile) of the feed sample had a particle size lower than 110.96 μm whereas after the micro-filtration this value was reduced up to 0.66 μm.

3.2. Permeability coefficients for the tested membranes

Table 3 shows for each membrane the linear regression that represent the influence of TMP on distilled water permeate flux, J_{cw} (L m^{-2} h^{-1}). The slope of each linear equation is the permeability coefficient of the membrane (L m^{-2} h^{-1} MPa^{-1}). The *R*-squared (R^2) that describes the quality of the regression is also presented.

Permeability values for the membranes TFC-SR2, Duraslick and DS-5 DK agree with those reported in previous research works [41].

It can be observed that all tested membranes have similar permeability coefficients with the exception of DS-5 DK and TFC-SR2. The first one has the lowest permeability coefficient (30 L m^{-2} h^{-1} MPa^{-1}) while the other one has the highest value (180 L m^{-2} h^{-1} MPa^{-1}). This agrees with the Hagen–Poiseuille equation (Eq. (5)).

$$J = \frac{r_p^2 \cdot \text{TMP}}{8 \cdot \mu \cdot (\Delta x / A_k)} \quad (5)$$

In this equation μ (kg m^{-1} s^{-1}) represents the dynamic viscosity of the solution, r_p is the pore radius and $\Delta x/A_k$ is the thickness–porosity ratio.

In this way, DS-5 DK membrane needs higher pressures to achieve permeate fluxes similar to the rest of membranes, especially TFC-SR2.

In the same table it is included the J_{cw} values calculated for the operating TMP of each membrane. As commented in Section 2.5, the operating TMP corresponds to a membrane recovery of 15% working with wastewater. These values have been calculated to determine normalised flux. The normalised flux is a relative flux (J_{ww}/J_{cw}) that is related to the effect of fouling generated by the organic and inorganic matter on the membrane flux reduction [17,27]. Thus, a ratio near 1 means a low influence of the wastew-

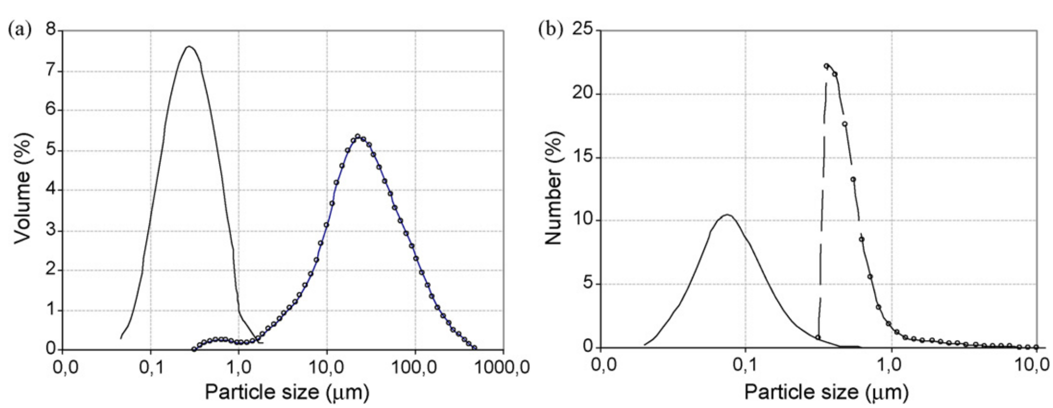

Fig. 2. Particle size distribution. (a) Measurements in volume and (b) measurements in number. (◯) Before MF (10 μm); (—) After MF (10 μm).

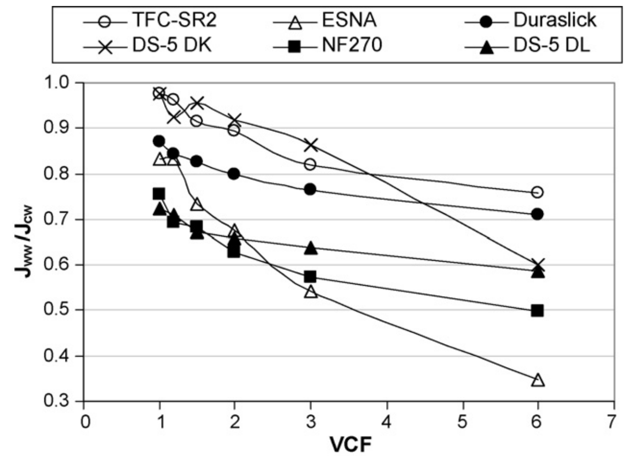

Fig. 3. Influence of VCF on the J_{ww}/J_{cw} ratio for the tested membranes.

ater solutes on the membrane behaviour, whereas a ratio near 0 represents a high influence level of them.

3.3. Influence of VCF on normalised flux

Fig. 3 depicts the influence of VCF on the normalised flux for the six tested membranes. As stated above, membrane fouling is evaluated by the normalised flux decline for each VCF. As expected, the membrane fouling was more severe for higher VCF values due to the increase of feed concentration. However, different behaviours of the tested membranes were registered.

It can be observed that at VCF = 1 the normalised flux was near 1 for two membranes: TFC-SR2 and DS-5 DK. For Duraslick and ESNA membranes the J_{ww}/J_{cw} parameter ranged between 0.82 and 0.88. On the contrary, NF270 and DS-5 DL were the most affected by the initial feed concentration. In these cases, the normalised flux was 0.75 and 0.70, respectively.

Although the tendency of normalised flux with the VCF is similar for all the membranes tested, it can be seen that the lowest flux reductions were also achieved by TFC-SR2. In fact, at the maximum VCF the normalised flux was over 0.77. It means, for this membrane, that the solute concentration in the feed water slightly affected the membrane flux.

Although the DS-5 DK presented the highest normalised flux values for VCF lower than 6, at VCF = 6 the flux reduction was pronounced and the final value reached (60%) means a total normalised flux decline of 40%. On the contrary, the ESNA membrane presented the highest reduction in terms of the depicted parameter; at VCF = 6 the normalised flux was 35%.

In order to explain these results, it is necessary to consider the membrane characterization parameters collected in the Table 1, especially the contact angle and the roughness.

Contact angle is a semi-quantitative index associated to the hydrophilicity/hidrophobicity of the membrane surface. The lower contact angle, the higher hydrophilicity and fouling tendency decreases [27,24]. In this way, it seems that TFC-SR2 presented a larger resistance to fouling because of its low contact angle value 13.1°. On the contrary, ESNA has the highest value (60.0°) and therefore the major flux ratio reduction and maximum fouling.

Other parameter to be considered is the surface roughness. This parameter is a physical property that defines the surface morphology which is also connected with the fouling tendency [34,42,43].

Particularly, the ESNA membrane presented the maximum normalised flux decrease and the highest roughness value (55.00 nm). On the contrary, TFC-SR2 membrane showed the minimum normalised flux decrease and the smoothest surface (0.45 nm). This small roughness value allows confirming the lack of picks on the membrane surface (see Fig. 4) and, as a result, the difficulty for linking foulants.

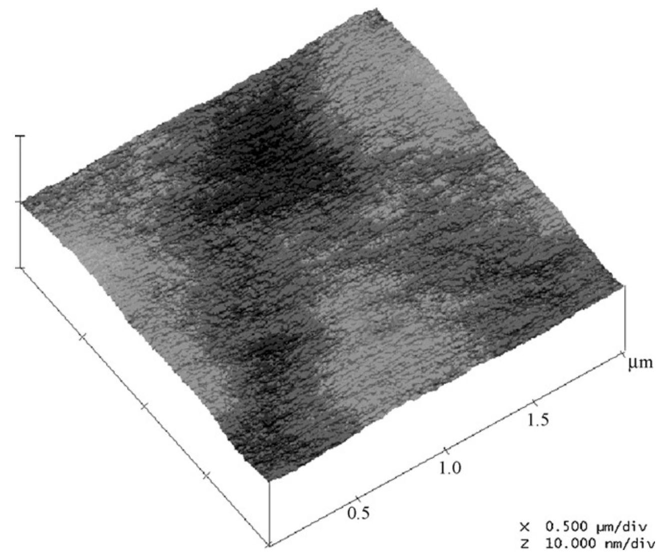

Fig. 4. AFM image of TFC-SR2 nanofiltration membrane.

Summarising, both contact angle and roughness values increased in the following order: TCF-SR2 < DS-5DK < Duraslick < DS-5DL < NF-270 < ESNA. Thus, it can be concluded that both contact angle and roughness values confirmed the fouling tendency showed by the membranes in the laboratory tests.

3.4. Influence of VCF on permeate flux

Fig. 5 represents for all membranes the J_{ww} values obtained at three different VCF (1, 3 and 6). The applied TMP for each membrane is also included.

In this figure, it can be observed that for the same membrane recovery (15%), the applied TMP differed considerably among the membranes. Thus, the TMP for TFC-SR2 and DS-5 DK membranes were 0.16 and 0.91 MPa, respectively. However, for these cases, the flux values were quite similar. On the other hand, the best J_{ww} values were achieved for Duraslick membrane. For this membrane the permeate flux varied between 27 and 33 L/(m^2 h) at a TMP = 0.53 MPa. Nevertheless, considering the lowest TMP applied and the moderate J_{ww} values obtained, the best membrane was the TFC-SR2.

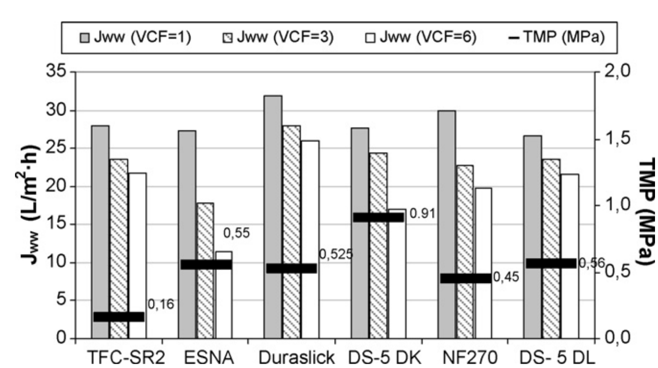

Fig. 5. J_{ww} values at different VCF and TMP applied for the tested membranes.

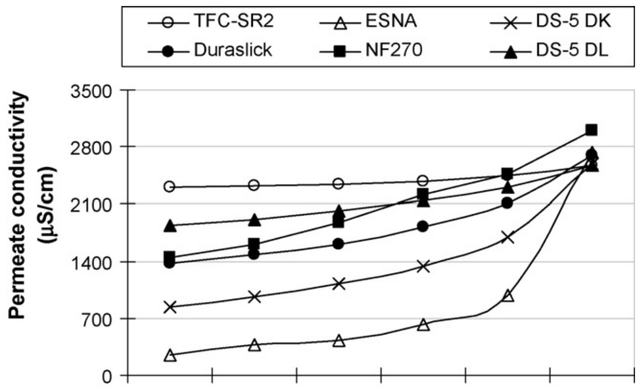

Fig. 6. Influence of VCF on permeates conductivity.

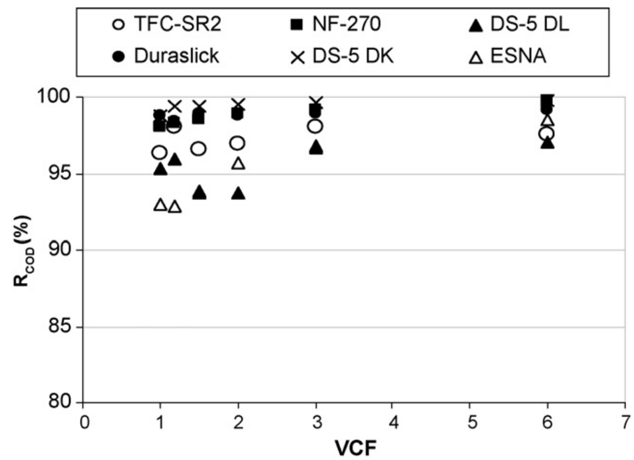

Fig. 8. Influence of VCF on COD rejection.

3.5. Influence of VCF on membrane rejection

3.5.1. Influence of VCF on salt rejection

In Fig. 6 the behaviour of the permeate conductivity with VCF for each membrane can be observed. In general, the permeate conductivity increased with VCF. In fact, the higher feed ion concentration, the higher solute pass through the membrane. It was not observed any fouling interference on salt pass.

Permeate conductivity values varied widely depending on the membrane tested. Hence, ESNA presented the lowest ones for all VCF except 6. Meanwhile, TFC-SR2 showed the highest values without observing significant variations independently of the VCF. This constant behaviour is explained because of the low salt rejection (30% for VCF = 6). These permeate conductivity values were mainly provided by monovalent ions. It suggests that the main retention mechanism was the size exclusion: membrane pore size (1.280 nm) and the ion hydrated diameter. Thus, the monovalent ions retention was negligible since the hydrated diameters values for Cl^- and Na^+ are 0.664 nm and 0.716 nm, respectively [44]. On the contrary, the ESNA membrane is the tightest membrane since the pore diameter is 0.6 nm, explaining in this way the high salt rejection (90% at VCF = 1 and 70% at VCF = 6).

With regard to divalent ions (Ca^{+2} and Mg^{+2}), the high rejection (between 90 and 98%) cannot only be attributed to the size exclusion, because the hydrated diameters are 0.824 nm and 0.856 nm for calcium and magnesium, respectively [44]. The explanation could be based on the Donnan effect (charge interactions) in which the divalent ions do not pass through the membrane in higher proportions to ensure the electroneutrality of the permeate stream and the value of the zeta potential (−21.8 at pH 8/10) [25].

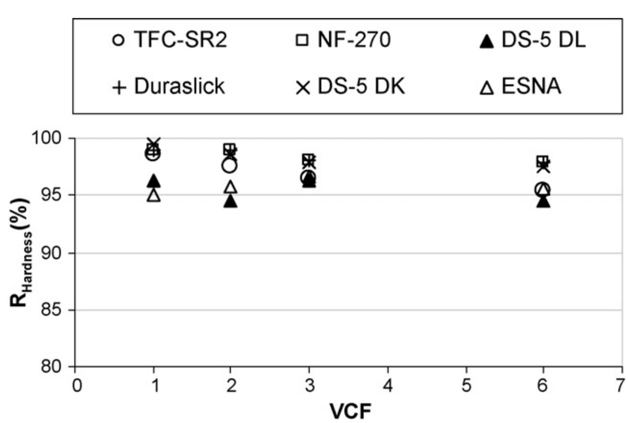

Fig. 7. Influence of VCF on hardness rejection.

However, these results suggest that the influence of the charge interactions on the separation was not relevant for all the tested membranes. In fact, operating pH was higher than the isoelectric points for all tested membranes. The zeta potential values at pH values near the wastewater pH indicated negative values for the zeta potential in the range from −5 to −24.7 mV in all cases. These values increase during the NF due to calcium ions absorption.

Thus, it can be stated that the differences in the behaviour of the membranes were based basically on the size exclusion.

The influence of the VCF on the hardness retention is described in the Fig. 7. The slight decrease was due to the diminution of the Donnan potential with the ions concentration [45].

3.5.2. Influence of VCF on COD and colour rejection

In general, an increase in VCF resulted in COD rejection increased (Fig. 8). This behaviour can be attributed to both the organic matter particle size and the fouling layer formed. COD rejection was high mainly due to the size differences between the pore membranes and organic matter. When the VCF was increased, fouling phenomena contributed to the COD removal enhancement. This fouling was formed by small particles that were not removed in the previous microfiltration (8 µm) of the feed.

The best COD rejections were achieved for ESNA 1 LF and NF270, obtaining COD concentrations in permeate stream lower than 20 mg L^{-1} at VCF = 6. These values together with hardness and conductivity data are summarized in Table 4. These results were in concordance with the pore size values.

Concerning colour rejection, it can be stated that the colour of the NF permeates was negligible in all the tests. Thus, independently from the membrane and from the VCF, colour removal was practically of 100%.

Dyes were completely removed since their molecular weight ranged 300–1000 Da and the tested membranes cut-off between 150 and 300 Da. Thus, during the experiments, there was no evidence of charge interactions between dyes and membranes that could enhance the dyes separation. In this way, neither colour

Table 4
COD, conductivity and hardness permeate values for tested membranes at VCF = 6.

Membrane	COD (mg L^{-1})	Conductivity (µS cm^{-1})	Hardness (mg L^{-1})
ESNA 1 LF	15	2740	6.69
NF270	15	3000	1.22
DS-5 DK	25	2590	3.77
DS-5 DL	25	2570	8.36
Duraslick	30	2700	3.21
TFC-SR2	25	2470	6.99

presence in permeate streams from membranes with lower pore diameter nor colour removal variation with the VCF were detected.

According to the results and to the quality requirements for the textile processes, the industrial feasibility of the permeate reuse has been proven out. Taking into account the operating conditions (TMP, VCF) and membrane fouling, it can be stated that the most appropriate membrane for this particular case is TFC-SR2. It has to be highlighted that this membrane is appropriate because the removal of monovalent ions is not necessary as can be checked in Table 1. This membrane meets the reuse criteria according to the measured parameters. Conductivity, hardness and COD rejection values were reported in Figs. 6–8, respectively. Besides, as explained above permeates colour, turbidity and TSS are negligible; thereby meet the reuse criteria equally.

4. Conclusions

For all membranes, the normalised flux declined with increasing VCF. However, important behaviour differences were found among the tested membranes. Thus, TFC-SR2 membrane showed the lowest fouling tendency whereas ESNA the highest one. According to the results obtained, difference in the membranes behaviour concerning normalised flux reduction was explained by the different contact angles and roughness. In general, it was observed the following tendency: the highest contact angle and roughness, the most marked fouling tendency.

For the TFC-SR2, it was possible to achieve the highest wastewater permeate flux at the lowest TMP applied with general recovery around 15%.

The tested membranes showed a lower monovalent ions rejection and a very high rejection for divalent ones. However, some differences were also observed among membranes. The differences were explained considering the size exclusion (pore size and ion hydrated diameter) and Donnan effects. In this way, ESNA presented the lowest permeates conductivity values and its separation mechanism is mainly due to the size exclusion whereas TFC-SR2 showed the lowest one and its separation mechanism is a combination of both size exclusion and Donnan effect, for most of the VCF tested.

In addition, for all VCF tested, the membranes removed completely the colour from the wastewater stream. No significant differences were observed in the colour measurements after the membrane experiments.

From the point of view of permeate quality all the tested membranes accomplished the reuse criteria. However, the high normalised flux at low TMP together with the minimum fouling made the TFC-SR2, the most appropriated membrane for the reclamation of the secondary textile wastewater and its reuse in the rinsing process.

Overall, it can be said that the results obtained have important implications for the environment, since a significant reduction of water and energy consumption is achieved by lower TMP.

Further tests have to be carried out in order to study the membrane behaviour at long-term experiments.

Acknowledgements

This work was supported by Ministerio de Educación y Ciencia (CTM2007-64451-AR07). We also thank Colortex 1967 S.L. for the textile wastewater samples and the technicians from the Microscope services from UPV for their support in AFM analysis.

References

[1] A. Bes-Piá, J.A. Mendoza-Roca, M.I. Alcaina-Miranda, A. Iborra-Clar, M.I. Iborra-Clar, Combination of physico-chemical treatment and nanofiltration to reuse wastewater of a printing, dyeing and finishing textile industry, Desalination 157 (2003) 73–80.
[2] A. Caniço-Gomes, I. Cabral-Gonçalves, M. Norberta de Pinho, The role of the adsorption on nanofiltracion of azo dyes, J. Membr. Sci. 255 (2005) 157–165.
[3] A. Bes-Piá, J.A. Mendoza-Roca, L. Roig-Alcover, A. Iborra-Clar, M.I. Iborra-Clar, M.I. Alcaina-Miranda, Comparison between nanofiltration and ozonation of biologically treated textile wastewater for its reuse in the industry, Desalination 157 (2003) 81–86.
[4] B. Van der Bruggen, E. Curcio, E. Drioli, Process intensification in the textile industry: the role of membrane technology, J. Environ. Manage. 73 (2004) 267–274.
[5] K. Boussu, C. Kindts, C. Vandecasteele, B. Van der Bruggen, Applicability of nanofiltration in the carwash industry, Sep. Purif. Technol. 54 (2007) 139–146.
[6] M. Mänttäri, K. Viitikko, M. Nyström, Nanofiltration of biologically treated effluents from the pulp and paper industry, J. Membr. Sci. 272 (2006) 152–160.
[7] L.M. Ortega, R. Lebrun, I.M. Noël, M.V. Hausler, Application of nanofiltration in the recovery of chromium (III) from tannery effluents, Sep. Purif. Technol. 44 (2005) 45–52.
[8] M.V. Galiana-Aleixandre, A. Iborra-Clar, A. Bes-Piá, J.A. Mendoza-Roca, B. Cuartas-Uribe, M.I. Iborra-Clar, Nanofiltration for sulphate removal and water reuse of the pickling and tanning processes in a tannery, Desalination 179 (2005) 307–313.
[9] A. Bes-Piá, B. Cuartas-Uribe, J.A. Mendoza-Roca, M.V. Galiana-Aleixandre, M.I. Iborra-Clar, M.I. Alcaina-Miranda, Pickling wastewater reclamation by means of nanofiltration, Desalination 221 (2008) 225–233.
[10] J.J. Qin, M.H. Oo, K.A. Kekre, Nanofiltration for recovering wastewater from a specific dyeing facility, Sep. Purif. Technol. 56 (2007) 199–203.
[11] A. Akbari, S. Desclaux, J.C. Rouch, P. Aptel, P.C. Remigy, New UV-photografted nanofiltration membranes for the treatment of colored textile dye effluents, J. Membr. Sci. 286 (2006) 342–350.
[12] I. Koyuncu, D. Topacik, M.R. Wiesner, Factors influencing flux decline during nanofiltration of solutions containing dyes and salts, Water Res. 38 (2004) 432–440.
[13] J.H. Mo, Y.H. Lee, J. Kim, J.Y. Jeong, J. Jegal, Treatment of dye aqueous solutions using nanofiltration poliamide composite membranes for the dye wastewater reuse, Dyes Pigments 76 (2007) 429–434.
[14] A. Akbari, J.C. Remigy, P. Aptel, Treatment of textile dye effluent using a polyamide-based nanofiltration membrane, Chem. Eng. Processing 41 (2002) 601–609.
[15] H.Z. Wu, Y.L. Hsu, Y.J. Lee, P.P. Lin, Reclamation of textile dyeing wastewater for process use via a highly efficient integration system, Desalination 172 (2005) 293–307.
[16] L. De Florio, A. Giordano, D. Mattioli, Nanofiltration of low-contaminated textile rinsing effluents for on-site treatment and reuse, Desalination 181 (2005) 283–292.
[17] A. Aouni, C. Fersi, M.B.S. Ali, M. Dhahbi, Treatment of textile wastewater by a hybrid electrocoagulation/nanofiltration process, J. Hazard. Mater. 168 (2009) 868–874.
[18] E. Sahinkaya, N. Uzal, U. Yetis, F.B. Dilek, Biological treatment and nanofiltration of denim textile wastewater for reuse, J. Hazard. Mater. 153 (2008) 1142–1148.
[19] R. Zylla, J. Sójka-Ledakowicz, E. Stelmach, S. Ledakowicz, Coupling of membrane filtration with biological methods for textile wastewater treatment, Desalination 198 (2006) 316–325.
[20] S. Barredo-Damas, M.I. Alcaina-Miranda, M.I. Iborra-Clar, A. Bes-Piá, J.A. Mendoza-Roca, A. Iborra-Clar, Study of the UF process as pretreatment of NF membranes for textile wastewater reuse, Desalination 200 (2006) 745–747.
[21] C. Fersi, M. Dhahbi, Treatment of textile plant effluent by ultrafiltration and/or nanofiltration for water reuse, Desalination 222 (2008) 263–271.
[22] S. Platt, M. Nyström, A. Bottino, G. Capannelli, Stability of NF membranes under extreme acidic conditions, J. Membr. Sci. 239 (2004) 91–103.
[23] J. Geens, K. Peeters, B. Van der Bruggen, C. Vandecasteele, Polymeric nanofiltration of binary water–alcohol mixtures: influence of feed composition and membrane properties on permeability and rejection, J. Membr. Sci. 255 (2005) 255–264.
[24] D. Norberg, S. Hong, J. Taylor, Y. Zhao, Surface characterization and performance evaluation of commercial fouling resistant low-pressure RO membranes, Desalination 202 (2007) 45–52.
[25] A.I. Schafer, A. Pihlajamaki, A.G. Fane, T.D. Waite, M. Nystrom, Natural organic matter removal by nanofiltration: effects of solution chemistry on retention of low molar mass acids versus bulk organic matter, J. Membr. Sci. 242 (2004) 73–85.
[26] Y. Shim, H.J. Lee, S. Lee, S.H. Moon, J. Cho, Effects of natural organic matter and ionic species on membrane surface charge, Environ. Sci. Technol. 36 (2002) 3864–3871.
[27] J. Tanninen, M. Mänttäri, M. Nyström, Effect of salt mixture concentration on fractionation with NF membranes, J. Membr. Sci. 283 (2006) 57–64.
[28] K. Boussu, C. Vandecasteele, B. Van der, Bruggen, Relation between membrane characteristic and performance in nanofiltration, J. Membr. Sci. 310 (2008) 51–65.
[29] L.D. Nghiem, P.J. Coleman, NF/RO filtration of the hydrophobic ionogenic compound triclosan: transport mechanisms and the influence of membrane fouling, Sep. Purif. Technol. 62 (2008) 711–718.
[30] J. Tanninen, S. Platt, A. Weis, M. Nystrom, Long-term acid resistance and selectivity of NF membranes in very acidic conditions, J. Membr. Sci. 240 (2006) 11–18.

[31] R. Liikanen, H. Kiuru, J. Peuravuori, M. Nystrom, Nanofiltration flux, fouling and retention in filtering dilute model waters, Desalination 175 (2005) 97–109.
[32] C. Tang, V. Chen, Nanofiltration of textile wastewater for water reuse, Desalination 143 (2002) 11–20.
[33] A.I.C. Morao, A.M.B. Alves, M.D. Afonso, Concentration of clavulanic acid broths: Influence of the membrane surface charge density on NF operation, J. Membr. Sci. 281 (2006) 417–428.
[34] N. Park, B. Kwon, I.S. Kim, J. Cho, Biofouling potential of various NF membranes with respect to bacteria and their soluble microbial products (SMP): characterizations, flux decline, and transport parameters, J. Membr. Sci. 258 (2005) 43–54.
[35] L.D. Nghiem, D. Vogel, S. Khan, Characterising humic acid fouling of nanofiltration membranes using bisphenol A as a molecular indicator, Water Res. 42 (2008) 4049–4058.
[36] D.X. Wang, M. Su, Z.Y. Yu, X.L. Wabg, M. Ando, T. Shintani, Separation performance of a nanofiltration membrane influenced by species and concentration of ions, Desalination 175 (2005) 219–225.
[37] G. Bargeman, J.M. Vollenbroek, J. Straatsma, C.G.P.H. Schroën, R.M. Boom, Nanofiltration of multicomponent feeds. Interactions between neutral and charged components and their effect on retention, J. Membr. Sci. 247 (2005) 11–20.
[38] American Public Health Association, American Water Works Association, Water Pollution Control Federation, in: S.A. Díaz Santos (Ed.), Standard Methods for Examination of Water and Wastewater, APHA/AWWA/WPCF, Madrid, España, 1992.
[39] E. Döpkens, R. Jonas, T. Jung, R. Krull, Rückführung von Abwasserteilströmen der Textilweredlung in den Produktionsprozess, in: GVC (Hrsg.), Proc. Colloquium Produktionsintegrierte Wasser-/Abwassertechnik, “Nachhaltige Produktion in der textilveredelung” und “Membrantechnik”, Bremen, 2001, B143–B157.
[40] C.I. Pearce, J.R. Lloyd, J.T. Guthrie, The removal colour from textile wastewater using whole bacterial cells: a review, Dyes Pigments 58 (2003) 179–196.
[41] A. Bes-Piá, A. Iborra-Clar, C. García-Figueruelo, S. Barredo-Damas, M.I. Alcaina-Miranda, J.A. Mendoza-Roca, M.I. Iborra-Clar, Comparison of three NF membranes for the reuse of secondary textile effluents, Desalination 241 (2009) 1–7.
[42] C. Hobbs, S. Hong, J. Taylor, Effect of surface roughness of RO and NF membranes during filtration of a high organic surficial groundwater, J. Water Supply: Res. Technol. AQUA 55 (2006) 166–178.
[43] E.M. Vrijenhoek, S. Hong, M. Elimelech, Influence of membrane surface properties on initial rate of colloidal fouling of reverse osmosis and nanofiltration membranes, J. Membr. Sci. 188 (2001) 115–128.
[44] Y. Marcus, Ion Solvation, Wiley, New York, 1985.
[45] B. Van der Bruggen, B. Daems, D. Wilms, C. Vandecasteele, Mechanisms of retention and flux decline for the nanofiltration of dye baths from the textile industry, Sep. Purif. Technol. 22 (2001) 519–528.